



Collision cascades in metals and semiconductors: defect creation and interface behavior

K. Nordlund^{a,b,*}, R.S. Averback^a

^a *Materials Research Laboratory, University of Illinois, Urbana, IL 61801, USA*

^b *Accelerator Laboratory, University of Helsinki, P.O. Box 43, FIN-00014, Helsinki, Finland*

Abstract

Using molecular dynamics simulations of collision cascades, we examine point defect and defect cluster formation mechanisms in metals and semiconductors. In metals we find that the primary mechanism causing separation of interstitials and vacancies is the pushing of vacancies toward the cascade center during the cooling phase of the cascade. We further describe how the isolation of a part of the liquid formed in the cascade can lead to the formation of interstitial clusters in metals. By comparing ballistically similar pairs of metals and semiconductors like Al and Si and Cu and Ge, we deduce how the cascade behavior depends on the nature of interatomic bonding and crystal structure. We also find that close to sharp interfaces of metals with different melting points the ‘vacancy push’ mechanism can lead to most vacancies being pushed to one of the materials, and an asymmetry in the impurity introduction over the interface owing to an inverse Kirkendall effect. © 2000 Elsevier Science B.V. All rights reserved.

PACS: 61.80.Jh; 61.72.Cc; 61.72.Ji; 61.72.Nn

1. Introduction

The effects of ion irradiation on metals and semiconductors have been extensively studied over more than four decades [1,2]. Despite this, some fundamental aspects of the development of collision cascades have started to become clear only fairly recently by the use of molecular dynamics (MD) simulations of high-energy cascades [3–6]. These simulations have shown that local melting can have a crucial role in the development of cascades, leading to low damage production in dense metals and amorphization in semiconductors. In the vicinity of surfaces local melting can have an even more dramatic effect on the total damage production by the flow of hot liquid onto surfaces [7,8].

In the present paper we review some recent MD studies of high-energy collision cascades in bulk metals and semiconductors, focusing on defect and defect

cluster production mechanisms, and discuss how the results relate to experimental findings. The role of surfaces on damage production will be discussed in another paper in these proceedings [9].

In Section 2 we briefly recall our central simulation principles. In Section 3 we discuss point defect and defect cluster production mechanisms, and in Section 4 we compare results between semiconductors and metals. In Section 5 we show that the cascade dynamics can have interesting consequences at sharp metallic bilayer interfaces.

2. Simulation principles

The simulation methods used in the studies discussed here have been described in detail elsewhere [10,11], so we only recall the most central principles here. In simulating ‘bulk’ collision cascades, which correspond to the damage caused by isolated primary recoils produced by neutrons or MeV ions, we give a lattice atom recoil energy in a random direction in the lattice towards the center of the simulation cell. Heat is dissipated out from

* Corresponding author. Tel. +358-9 1914 0007; fax: +358-9 1914 0042.

E-mail address: kai.nordlund@helsinki.fi (K. Nordlund)

the simulation cell at the borders using Berendsen pressure control [12] at the outermost atom layers with an optimized time constant. The development of the system of atoms is followed using MD simulations until the cascade has cooled down close to the ambient temperature (usually 0 K). Varying the initial velocity direction and position of the recoil atom can cause the resulting cascades to behave quite differently (even for the same ion-energy-sample combination) depending on where the strongest collisions occur.

The interactions between atoms are treated with the embedded-atom method (EAM) potentials for metals [13] and Stillinger–Weber or Tersoff three-body potentials for silicon and germanium [14–16]. The equilibrium potentials are smoothly joined to the Ziegler–Biersack–Littmark repulsive interatomic potential [17] or *ab initio* dimer potentials [18] for small interatomic separations to treat energetic collisions realistically. The SRIM96 electronic stopping power [19] is taken into account as a frictional force affecting the motion of all atoms with a kinetic energy higher than 10 eV. We do not include a model for electron–phonon coupling since our recent comparison of simulated and experimental ion beam mixing values indicates that in the fcc metals treated here it does not affect the overall cascade development much [20].

We usually recognize defects using Wigner–Seitz cells/Voronoy polyhedra centered on the original lattice atom positions, labeling empty cells as vacancies and double filled cells as interstitials. In the analysis of amorphous regions in semiconductors this definition can be somewhat misleading, but in practice the number of Wigner–Seitz defects recognized in amorphous pockets will be proportional to the size of the region [10], so this definition can still be used as an estimate of the total amount of damage in the simulation cell.

The use of model potentials to describe a material does of course not necessarily guarantee that the results reflect the behavior of the real material. In the present case, however, the potentials used should give an adequate description of those material properties that are widely believed to be central for the development of collision cascades. The EAM potentials give a quite satisfactory description of the properties of melting, the liquid and solid state, elastic constants and defect diffusion of the metals [13]. For Si and Ge both the Stillinger–Weber and Tersoff potentials reproduce elastic constants and the nature of the covalent bonding well [21]. The Tersoff potential has some problems in describing melting of the material, which may cause problems in its description of amorphization [10]. In the present work, however, we focus on comparing cascade behavior in different materials. Although the interatomic potentials used have some inaccuracies in their description of each material, these are in almost all cases much smaller than the differences between the materials (both

in the models and in reality). Furthermore, the large difference between metals and semiconductors in their resolidification properties are primarily governed by the different bonding types, which are described well by the potentials [10,13,21,22]. Thus we believe that the present work gives an at least qualitatively correct picture of differences in the response of real materials to ion irradiation.

3. Defect production in metals

The present understanding of the overall development of collision cascades induced by keV heavy ions can be summarized as follows. In light materials with a low atomic density like aluminum and silicon, the cascades are roughly linear, and no large liquid zones form within the cascade. For instance in silicon the cascade development can in fact be rather well represented by binary collision approximation simulations, especially if the parameters in the simulation are calibrated with MD simulations [23]. In semiconductors like Si and Ge the regions of the crystal strongly disordered by the irradiation form amorphous zones upon cooling-down due to the low recrystallization rate of the materials [22]. In heavy dense metals, on the other hand, large liquid zones form during irradiation, but during the cooling-down phase of the cascade the crystal regenerates almost perfectly, and only a few isolated point defects remain after cooling [3,10] (see Fig. 1). With this overall structure in mind, we now discuss the point defect and defect cluster formation mechanisms.

The mechanism leading to the formation of vacancies and vacancy clusters in metals is quite well understood. The ejection of interstitials by replacement collision sequences (RCSs) or the formation of interstitial clusters at the outskirts of the cascade leads to a deficiency of atoms in the liquid region. When the liquid region solidifies [3], it has a strong tendency to recrystallize into a perfect crystal. Hence the empty volume in the liquid will be pushed towards the center of the cascade, where it will form a loose network of single vacancies or a vacancy cluster.

In a recent comparison between simulated and experimental results on cascades in tungsten we found that at least in this material MD simulations reproduce the shape of this vacancy network quite well [24].

It has long been clear that isolated interstitials can be produced by replacement collision sequences in fcc and bcc metals [25,26]. This was frequently assumed to be the dominant mechanism separating interstitials from vacancies, thus preventing their recombination by low-temperature interstitial migration. Recent simulations have indicated, however, that RCSs are in fact rather short on average, so interstitials are mostly created close to the edge of the liquid zones of the cascades [10,27].

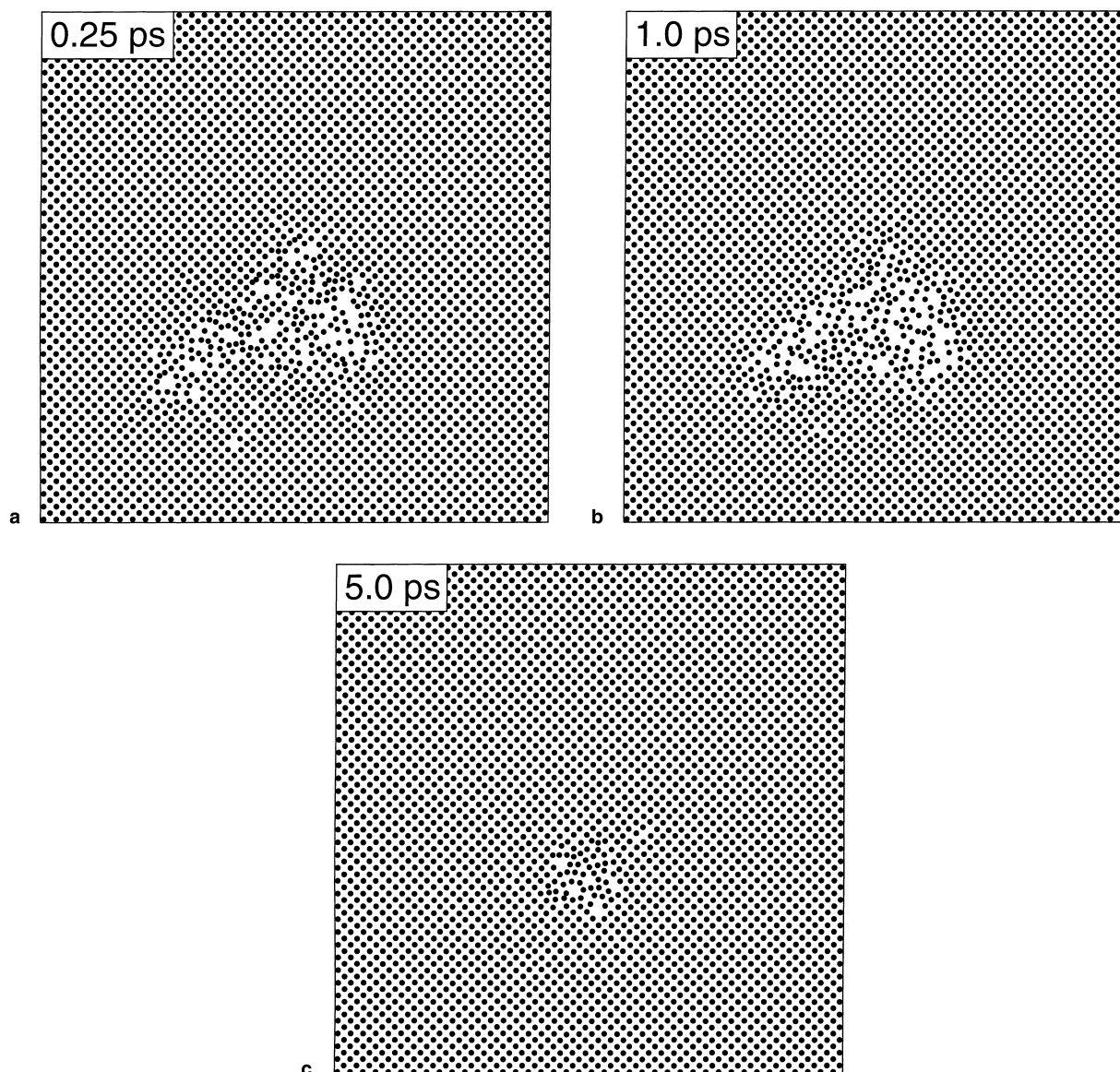


Fig. 1. Illustration of the development of a 10 keV cascade in the bulk in copper induced by a self-ion. Each dot shows the position of one atom in a slice with a thickness of one unit cell. Note that although the empty volume in the cascade is distributed almost evenly at 1 ps, most of the vacancies left at 5 ps (when the crystal has regenerated almost completely) are in the central region of the simulation cell. From Ref. [8].

Hence the ‘vacancy push’ effect in cascade cores described above emerges as an important factor leading to interstitial-vacancy separation in high-energy cascades.

While the mechanism forming vacancy clusters is relatively well understood, the mechanisms producing interstitial clusters in bulk cascades have long remained unclear. While clusters have been observed to be produced directly in collision cascades [27], the mechanism leading to cluster formation is not clear. A ‘loop punching’ mechanism by coherent atom displacement

has been proposed to be active [28], but this has not been clearly established [7,29].

We have compared the initial and final positions of displaced atoms in a large number of 10 and 50 keV collision cascades in fcc metals, analyzing the formation of all interstitial clusters containing more than ≥ 10 Wigner–Seitz defects, but none of these were found to form by loop punching. We have, however, observed another mechanism leading to interstitial cluster formation. A part of the liquid zone produced by the

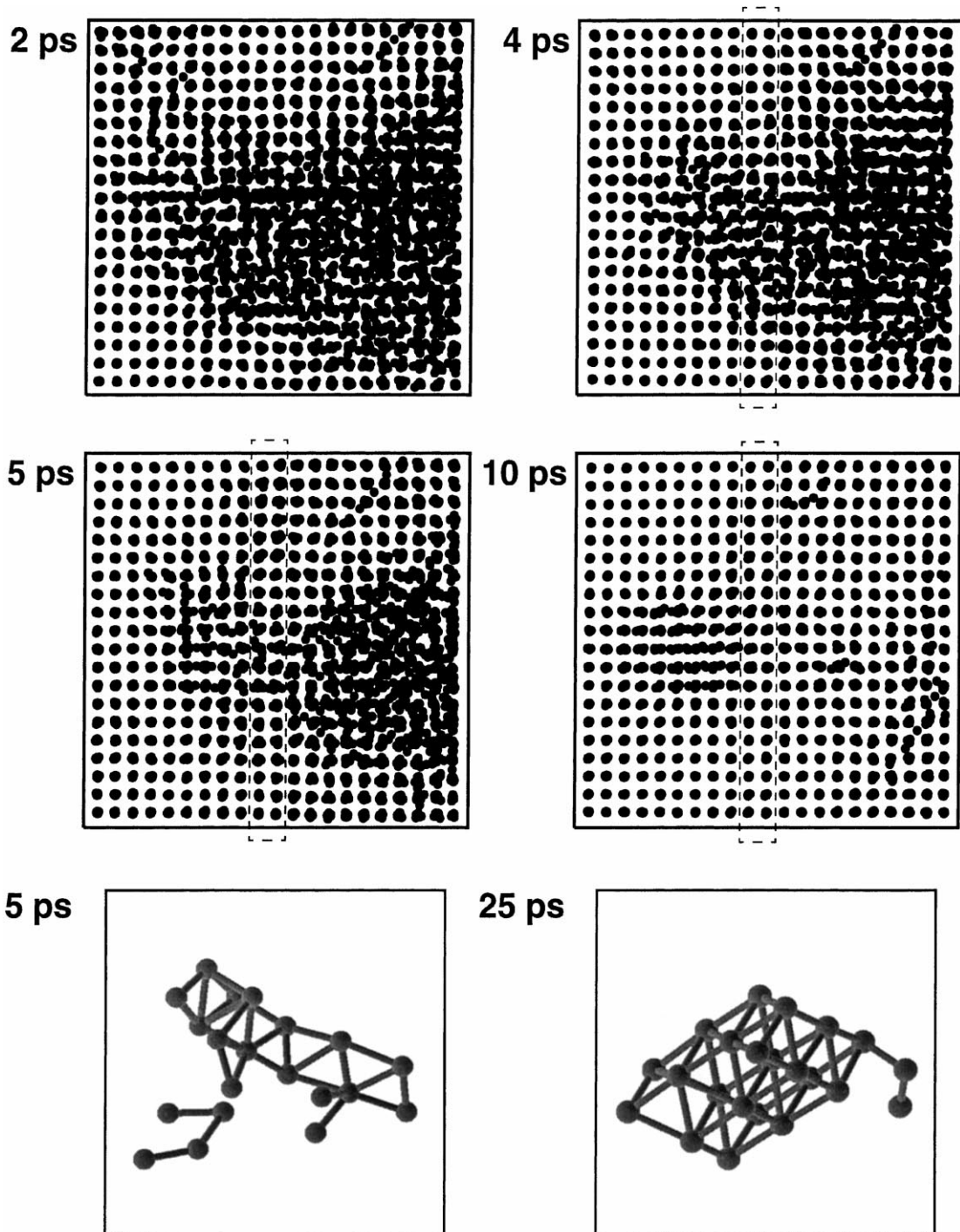


Fig. 2. Formation of a defect cluster in a 10 keV cascade in Pt. The top four figures show the atom positions in a $40 \times 40 \times 50 \text{ \AA}$ region of the simulation cell projected onto the xy plane. The two atom rows which crystallize and isolate part of the liquid are highlighted with a dashed rectangle. The lowest figures show the positions of atoms in the cluster at 5 and 25 ps. From Ref. [10].

cascade can be isolated by the formation of a recrystallized ‘neck’ in the liquid. If the isolated part of the liquid contains too many atoms (which is quite likely to

occur since the high pressure in the central region tends to push atoms towards the outskirts of the liquid), the recrystallization of the neck prevents the interstitials

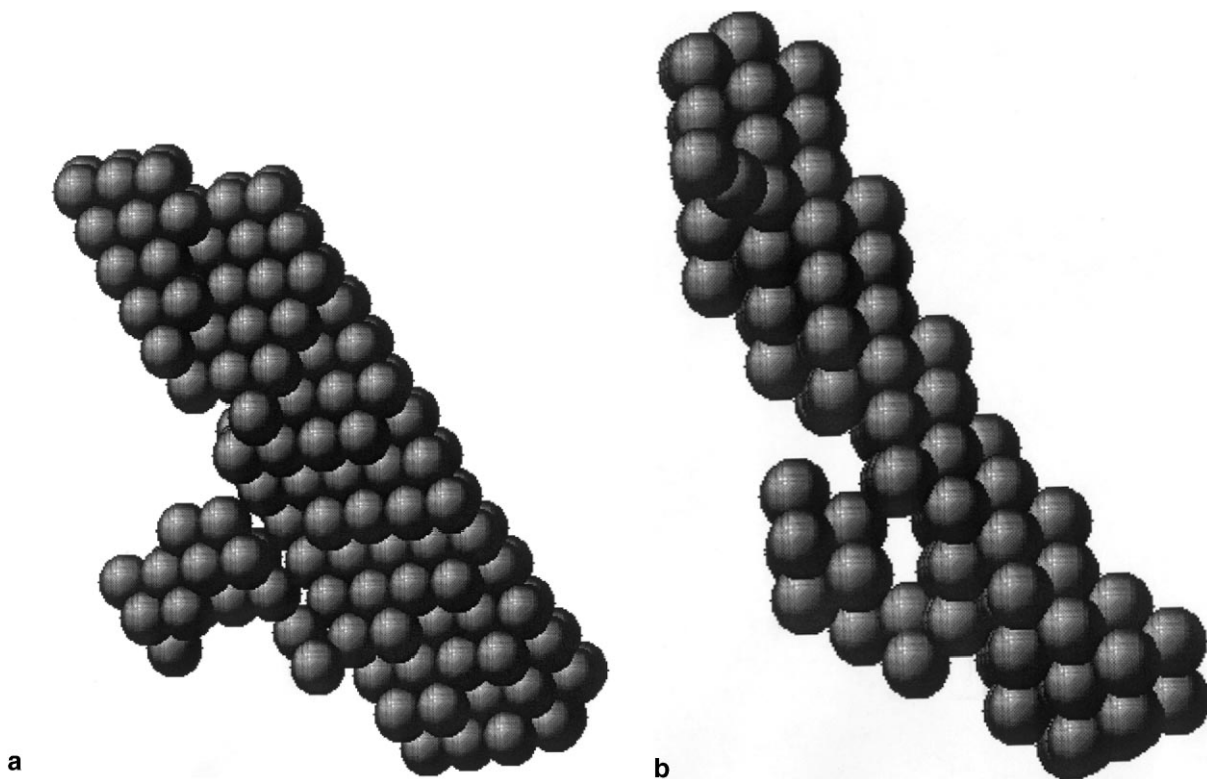


Fig. 3. Interstitial cluster produced in a 50 keV collision cascade in copper, seen from two different directions. Each sphere shows the final position of each atom in the cluster. The central cluster consists of a number of $\{111\}$ atom platelets partially on top of each other.

from collapsing inwards towards the center of the cascade, leading to the formation of an interstitial cluster. The mechanism is illustrated in Fig. 2.

Detecting the liquid isolation mechanism is not straightforward, whence we have not unambiguously recognized it in many events. Most of the interstitial clusters seen tend to form at the outer regions of the liquid zones of the cascades, however, which is consistent with this mechanism.

Since the interstitial cluster is formed from the liquid, its initial shape is rather disordered (see the lower part of Fig. 2). But while the cascade cools-down, the temperature around the center of the cell is still sufficiently high to allow for reorganization of the interstitial atoms. The final shape of the interstitial cluster, some 25 ps after initiation of the cascade, already shows quite well-defined side facets.

Analysis of five 50 keV cascades induced by self-ions in bulk Cu and Ni, showed that even larger, rather well-ordered interstitial clusters can form directly in the collision cascade. The final shape of the largest one (containing about 150 atoms) is illustrated in Fig. 3. The size of clusters formed in the other bulk events varied widely, but on average the size of the largest interstitial

and vacancy cluster in both Ni and Cu was about 30 defects. The total number of defects in the same events was on average about 100. None of the clusters formed had a perfect dislocation loop structure, but many of them consisted in part of well-formed platelets, even though the simulations were ended after the cascade had cooled down after about 30 ps. On experimentally accessible timescales it seems plausible that at least many of these defect clusters would collapse into regularly shaped loops or stacking fault tetrahedra.

The experimental difference between damage production in Ni and Cu during neutron irradiation, corresponding to cascades not affected by surfaces, is roughly a factor of ~ 1.5 [30–35]. Although it is not quite clear whether this difference is related to low-temperature defect migration, the result has not been observed to depend strongly on temperature, so we can attempt to compare the result with MD simulations. The average damage production in our simulations does not differ much, but the largest clusters seem to be produced in the Cu events. With only 5 events simulated in each material, this can of course only be a statistical variation. But the difference would be consistent with the observation that the liquid zone in Cu cascades is larger

than in Ni [10], so it can be expected to lead to the formation of larger clusters. The experimental difference might also be related to an electron-phonon coupling effect not affecting the mixing strongly.

4. Comparison between metals and semiconductors

We have compared the development of collision cascades in Al and Si on the one hand, and Cu and Ge on the other, to deduce how the crystal structure and bonding type affect the development of cascades [10]. Since these pairs of materials have similar atomic masses, their purely ballistic behavior is expected to be quite similar. Al and Si also have almost the same atomic density, whence differences between cascade behavior in them must primarily stem from the difference in crystal structure and bonding type.

Cascade development in typical semiconductor materials like Si and Ge is in some respects quite different than that in metals. The open diamond crystal structure leads to medium-energy secondary recoils traveling considerably longer than in metals with a similar atomic density [36]. This explains why the ion beam mixing in semiconductors tends to be higher than in metals [37,38] and leads to dilute cascades in semiconductors [10].

Interstitials in silicon are not created by well-defined RCS's as in metals [39]. Instead they are formed by low-energy recoils traveling typically 4–7 Å [10]. The distances from the interstitials to the nearest vacancy, however, is about 15 Å, almost exactly the same as in aluminum. Thus, even though the mechanisms forming interstitials are rather different, their final distribution is not that different.

The largest difference between the initial state of damage lies in how the central liquid zone of the cascade solidifies. As we have seen above, in metals the cascade tends to regenerate into perfect crystal except for a few vacancies left behind in the central zone of the cascade. In Si and Ge, by contrast, the recrystallization velocity is so low that during the very rapid cooling in a collision cascade the liquid or disordered region formed in the cascade does not have time to reorder into crystalline material. Instead, it is left in an amorphous state [5,22]. The total amount of damage (counted as disordered Wigner–Seitz cells, defect spheres or simply atoms in the amorphous zones [10]) will be much larger in semiconductors. This is illustrated in Fig. 4, which shows the distribution of defects produced by self-recoils in clusters of various sizes. Note that the abscissa scales in the Si and Al figures differ by an order of magnitude. The clusters, or amorphous zones, are dramatically larger in Si than in Al.

5. Heat spikes at bilayer interfaces

The ‘vacancy push’ effect described above can have interesting consequences at metallic bilayer interfaces. Consider a collision cascade centered at a sharp bilayer interface between, for instance, Ni and Cu. Since Ni has a much higher melting point than Cu (1730 K vs. 1360 K for Cu), the liquid zone formed in it is much smaller than that in Cu, and resolidifies much faster [10]. Since interstitials are created normally, however, the liquid in Ni has some empty volume. As the Ni crystal strives to regenerate, the empty volume in it will be pushed over to the Cu side of the interface. Thus almost all the vacancies will end up in Cu. But since there are too few Ni

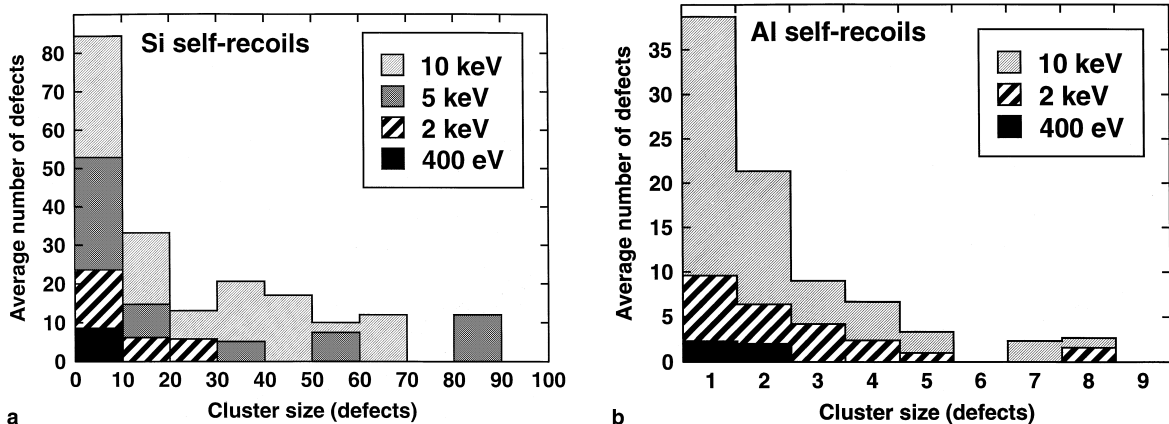


Fig. 4. Distribution of Wigner–Seitz defects as a function of the cluster size for Si (a) and Al (b), measured as the number of Wigner–Seitz defects each cluster contains. The data for each energy are overlaid on that of the higher energies. The numbers are the average over 6–10 events for each energy. Because of the limited number of events and clusters produced by them, the upper end of the 2–10 keV distributions are not statistically significant. From Ref. [10].

Table 1

Average defect results of the 5 keV collision cascades close to a Co/Cu or Co/Ni interface^a

	Cu _{Co/Ni}	Co/Ni _{Cu}	I _{Cu}	I _{other}	V _{Cu}	V _{Co/Ni}
Co/Cu	17.3	13.6	5.7	6.9	9.3	3.3
Co/Ni	29	23	9.5	6.5	14.7	1.3

^a Cu_{Co/Ni} denotes Cu impurities in Co or Ni, Co/Ni_{Cu} Co or Ni impurities in Cu, I_{Co/Ni} interstitials in Co or Ni and V_{Co/Ni} vacancies in Co or Ni. 16 events were simulated in the Cu/Co system and 6 in the Cu/Ni system. From Ref. [40].

atoms, the vacant sites in Ni (just before they are pushed over into Cu) will be filled with Cu atoms. This will lead to more Cu impurities in Ni than vice versa.

We detected the mechanism outlined above by simulating 5 keV cascades at Cu/Ni and Cu/Co {1 1 1} interfaces [40]. To prevent ballistic effects from biasing the results, the recoils were started from random locations on both sides of the interface, but directing them towards it. The results are summarized in Table 1. As outlined above, most vacancies are in Cu, and there are more Cu impurities in Co or Ni than vice versa. The final distribution of vacancies and impurities after one event is illustrated in Fig. 5.

The behavior described above can be summarized as a vacancy flux driving an impurity flux in the opposite direction over an interface, that is, it is analogous to the inverse Kirkendall effect known to occur during radiation enhanced diffusion [41]. Since in this case the driving force is quite different than in the classical effect, however, we prefer to interpret it as a new kind of

Kirkendall effect, inverse Kirkendall mixing in collision cascades.

6. Conclusions

The results discussed in the present paper have shown that many aspects of cascade development in the bulk have been much clarified by the systematic use of MD simulations. The role of heat spikes in metals starts to be fairly clear, and in particular the pushing of empty volume in cascades towards the cascade center has been found to have many interesting consequences. It appears to be an important factor causing separation of vacancies and interstitials, and it can lead to the formation of vacancy clusters and loops in high-energy cascades. Furthermore, the effect was also found to lead to an imbalance in the defect and impurity distribution at sharp metallic bilayer interfaces.

The results also demonstrated one mechanism leading to interstitial clustering, the isolation of a liquid pocket with an excess of atoms, which then forms an interstitial cluster during cooling. Further study is needed, however, to determine whether this is the dominant mechanism, or whether other mechanisms can be active as well. In 50 keV bulk cascades in Cu and Ni we observed the formation of large clusters of both interstitial and vacancy character, sometimes containing around 100 atoms and having dimensions of 2–4 nm.

The comparison of cascade development between silicon and aluminum showed that isolated interstitials are distributed in a roughly similar manner in both materials, but that the nature of the damage produced is otherwise quite different due to the formation of amorphous pockets in silicon.

Acknowledgements

The research was supported by the Academy of Finland and the US Department of Energy, Basic Energy Sciences under grant DEFG02-91ER45439. Grants of computer time from the National Energy Research Computer Center at Livermore, California, the National Center for Supercomputing Applications in Champaign, Illinois, and the Center for Scientific Computing in Espoo, Finland, are gratefully acknowledged.

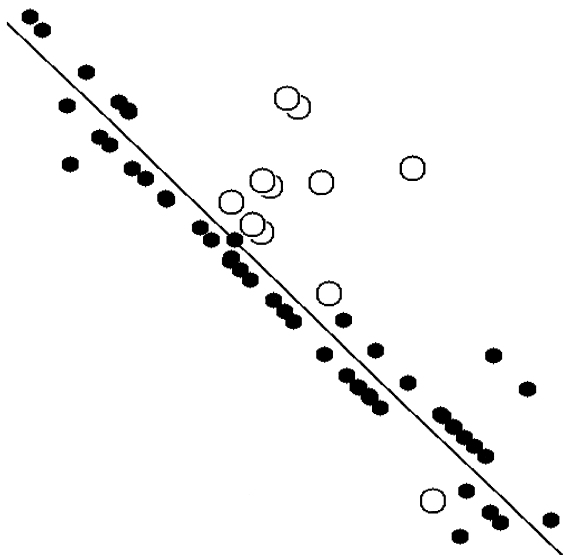


Fig. 5. Distribution of impurities and vacancies after one 5 keV event close to a Co/Cu interface. The line shows the position of the {1 1 1} interface, the filled circles the positions of impurities and the open circles the positions of vacancies. The Co part of the crystal is in the lower left part of the figure; thus all filled circles in this part are Cu impurities. From Ref. [40].

References

- [1] F. Seitz, J.S. Koehler, in: F. Seitz, D. Turnbull (Eds.), *Solid State Physics*, 2, Academic Press, New York, 1956, p. 307.
- [2] R.S. Averback, T. Diaz de la Rubia, in: H. Ehrenfest, F. Spaepen (Eds.), *Solid State Physics*, 51, Academic Press, New York, 1998, p. 281.
- [3] T. Diaz de la Rubia, R.S. Averback, R. Benedek, W.E. King, *Phys. Rev. Lett.* 59 (1987) 1930.
- [4] H. Hsieh, T. Diaz de la Rubia, R.S. Averback, R. Benedek, *Phys. Rev. B* 40 (1989) 9986.
- [5] T. Diaz de la Rubia, G.H. Gilmer, *Phys. Rev. Lett.* 74 (1995) 2507.
- [6] D.J. Bacon, A.F. Calder, F. Gao, *Radiat. Eff. Def. Solids* 141 (1997) 283.
- [7] M. Ghaly, R.S. Averback, *Phys. Rev. Lett.* 72 (1994) 364.
- [8] M. Ghaly, K. Nordlund, R.S. Averback, *Philos. Mag. A*, 1998, in press.
- [9] R.S. Averback, K. Nordlund, C.P. Flynn, presented at the Workshop on Basic Aspects of Differences in Irradiation Effects between FCC, BCC and HCP Metals and Alloys, Cangas de Onis, Spain, Oct. 1998.
- [10] K. Nordlund, M. Ghaly, R.S. Averback, M. Caturla, T. Diaz de la Rubia, J. Tarus, *Phys. Rev. B* 57 (1998) 7556.
- [11] K. Nordlund, R.S. Averback, *Phys. Rev. B* 56 (1997) 2421.
- [12] H.J.C. Berendsen, J.P.M. Postma, W.F. van Gunsteren, A. DiNola, J.R. Haak, *J. Chem. Phys.* 81 (1984) 3684.
- [13] M.S. Daw, S.M. Foiles, M.I. Baskes, *Mater. Sci. Rep.* 9 (1993) 251.
- [14] F.H. Stillinger, T.A. Weber, *Phys. Rev. B* 31 (1985) 5262.
- [15] J. Tersoff, *Phys. Rev. B* 39 (1989) 5566.
- [16] J. Tersoff, *Phys. Rev. B* 41 (1990) 3248.
- [17] J.F. Ziegler, J.P. Biersack, U. Littmark, *The Stopping and Range of Ions in Matter*, Pergamon, New York, 1985.
- [18] K. Nordlund, N. Runeberg, D. Sundholm, *Nucl. Instrum. Meth. Phys. Res. B* 132 (1997) 45.
- [19] J.F. Ziegler, 1996, SRIM-96 computer code, private communication.
- [20] K. Nordlund, L. Wei, Y. Zhong, R.S. Averback, *Phys. Rev. B (Rapid Commun.)* 57 (1998) 13965.
- [21] H. Balamane, T. Halicioglu, W.A. Tiller, *Phys. Rev. B* 46 (1992) 2250.
- [22] M.-J. Caturla, L.A.M.T. Diaz de la Rubia, G.H. Gilmer, *Phys. Rev. B* 54 (1996) 16683.
- [23] H.L. Heinisch, B.N. Singh, T. Diaz de la Rubia, *J. Nucl. Mater.* 212–215 (1994) 127.
- [24] Y. Zhong, K. Nordlund, M. Ghaly, R.S. Averback, *Phys. Rev. B (Brief Reports)* 58 (1998) 2361.
- [25] J.B. Gibson, A.N. Goland, M. Milgram, G.H. Vineyard, *Phys. Rev.* 120 (1960) 1229.
- [26] C. Erginsoy, G.H. Vineyard, A. Englert, *Phys. Rev.* 133 (1964) 595.
- [27] D.J. Bacon, T. Diaz de la Rubia, *J. Nucl. Mater.* 216 (1994) 275.
- [28] T. Diaz de la Rubia, M.W. Guinan, *Phys. Rev. Lett.* 66 (1991) 2766.
- [29] T. Diaz de la Rubia, *Nucl. Instrum. Meth. Phys. Res. B* 120 (1996) 19.
- [30] P. Ehrhart, R.S. Averback, *Philos. Mag. A* 60 (1989) 283.
- [31] Y. Shimomura, H. Yoshida, M. Kiritani, K. Kitagawa, K. Yamakawa, *J. Nucl. Mater.* 133&134 (1985) 385.
- [32] M. Kiritani, T. Yoshiie, S. Kojima, Y. Satoh, K. Hamada, *J. Nucl. Mater.* 174 (1990) 327.
- [33] M. Kiritani, *J. Nucl. Mater.* 155–157 (1988) 113.
- [34] J.A. Horak, T.H. Blewitt, *Phys. Stat. Sol.* 9 (1972) 721.
- [35] M. Rühle, *Phys. Stat. Sol.* 19 (1967) 279.
- [36] K. Nordlund, R.S. Averback, *Appl. Phys. Lett.* 70 (1997) 3103.
- [37] K. Nordlund, M. Ghaly, R.S. Averback, *J. Appl. Phys.* 83 (1998) 1238.
- [38] B.M. Paine, R.S. Averback, *Nucl. Instrum. Meth. Phys. Res. B* 7/8 (1985) 666.
- [39] M.-J. Caturla, T. Diaz de la Rubia, G.H. Gilmer, *Mater. Res. Soc. Symp. Proc.* 316 (1994) 141.
- [40] K. Nordlund, R.S. Averback, *Phys. Rev. B* 59 (1999) 20.
- [41] A.D. Marwick, *J. Phys.* (1978) 1849.